GEOLOGY | THE GEOLOGICAL SOCIETY OF AMERICA®

https://doi.org/10.1130/G45507.1

Manuscript received 20 August 2018
Revised manuscript received 25 January 2019
Manuscript accepted 6 March 2019

The largest delta plain in Earth's history

Tore Grane Klausen[1,2], Björn Nyberg[1], and William Helland-Hansen[1]
[1]Department of Earth Science, University of Bergen, Allégaten, 41, 5020 Bergen, Norway
[2]Petrolia NOCO AS, Espehaugen 32, 5836 Bergen, Norway

ABSTRACT

Delta plains host heavily populated and extensive agricultural areas with strong anthropogenic overprints on the natural evolution of these important landforms. Furthermore, modern delta plains have formed over a short geological time frame, representing immature end members to ancient counterparts in Earth's history—it could thus be argued that these are poor analogues for deciphering the sedimentary rock record. Our present study offers unique insight into the controls and potential extent of ancient deltas by investigation of the Triassic Boreal Ocean, where a large delta plain has been traced across >1.65 × 10^6 km^2. We show by comparison that the Triassic Boreal Ocean delta plain is larger than all modern and known ancient counterparts. Supply-driven progradation of this delta system proceeded uninterrupted on a 10^6 yr scale, indicating relative sea-level stability during this period—in support of a Triassic Greenhouse without pronounced glaciations. Reconstructed paleo-bathymetric relief shows the Triassic Boreal Ocean to have been one order of magnitude smaller than modern equivalents, explaining its vast extent. Despite its extent, the delta plain shows similar geomorphological characteristics to many modern delta plains, supporting their validity as analogues to the ancient, although scales might vary significantly.

INTRODUCTION

Understanding the character and development of delta plains is crucial to constraining past eustatic sea level (Haq et al., 1987; Miller et al., 2005), paleogeographic reconstructions (Miller et al., 2013), past climate (Hochuli and Vigran, 2010), and the evolution of life (Woodroffe et al., 2006; Greb et al., 2006). Our understanding of the nature and character of ancient deltaic depositional environments is complicated by how modern delta plains have developed in an anomalous Holocene highstand period with strong anthropogenic influence. For example, sediments trapped upstream by dams combined with bank-stability measures and a rising global sea level (Syvitski et al., 2009) result in net land loss downstream (Blum and Roberts, 2009)—directly affecting the shape of delta plains (Syvitski and Saito, 2007). With global sea level expected to rise (Rahmstorf, 2007) and delta plains continuing to subside (Syvitski et al., 2009), present geomorphological characteristics of deltas are being affected by extreme and anomalous effects of anthropogenic interference. Given that this interference is not counteracted, the present interglacial highstand could be sustained (Archer and Ganopolski, 2005) while deltas will be prevented from resuming the depositional style characterizing foregone periods with prolonged highstands, such as the Triassic, when low-gradient delta plains developed over the large marine areas that are today occupied by continental shelves.

To investigate the character and extent of a large-scale delta plain unaffected by human interaction, we use seismic reflection data and well logs to study the subsurface succession of the Triassic Boreal Ocean (TBO; Fig. 1). This succession is characterized by a large (hundreds-of-kilometers areal extent) deltaic river system of Carnian age (237–227 Ma) across the entire present-day Barents Sea and is also exposed in outcrops in islands along the uplifted northern flank of the basin (Klausen et al., 2015). We consider the overall extent of the TBO delta plain in relation to ancient and modern analogues, and discuss the exceptional circumstances required to produce the largest delta plain in Earth's history.

CHARACTERISTICS OF THE TRIASSIC BOREAL OCEAN DELTA PLAIN

A delta plain is defined as the coastal areas with a common gradient profile, controlled by backwater-length, toward a proximal knickpoint between the alluvial plain and the fluviatile to marine-influenced parts of river systems (Blum and Roberts, 2009; Bhattacharya et al., 2016). Siliciclastic sedimentation in the TBO started with very high sedimentation rates shortly after the Permian-Triassic event (Eide et al., 2017), resulting in kilometer-thick siltstone-dominated successions prograding >1000 km into the basin during the Induan (Early Triassic) and creating a relatively shallow epicontinental basin. After a reduction in sediment influx during the Olenekian and part of the Anisian, indicated by the slight backstepping of sedimentary packages relative to the Induan (Fig. 1C), sediment supply resurged in the Middle Triassic Ladinian interval. Because the northwestern boundary of this system cannot been defined, it is impossible to say how far the system prograded, but it had to prograde >500 km to cover the entire basin with deltaic sediment. This westward migration of its main depocenter could be explained by the Ladinian humid interval (Bernardi et al., 2018) and later Carnian pluvial events (Hochuli and Vigran, 2010) as possible climatic drivers that facilitated resurgence in sediment supply to the basin.

Semi-parallel subsurface seismic reflections are tied to specific periods within the Triassic according to biostratigraphic information (Vigran et al., 2014) and are traceable throughout the greater Barents Sea basin. Within the Middle to Upper Triassic (Ladinian to early Norian) Snadd Formation, each progradational package approximates 2–5 m.y. (Paterson and Mangerud, 2017), and within these discrete rock intervals, characteristic contrasts in acoustic properties enable identification of geomorphological features down to ~15 m thickness in three-dimensional (3-D) seismic data, and are used together with core and well logs to interpret fluvial and interbedded shallow marine depositional environments. Three-dimensional seismic data show large-scale channel belts up to 25 km wide and >50 m thick with pronounced lateral accretion surfaces in the eastern part of the basin, formed during the early Carnian interval (Fig. 2). This is

CITATION: Klausen, T.G., Nyberg, B., and Helland-Hansen,W., 2019, The largest delta plain in Earth's history: Geology, https://doi.org/10.1130/G45507.1

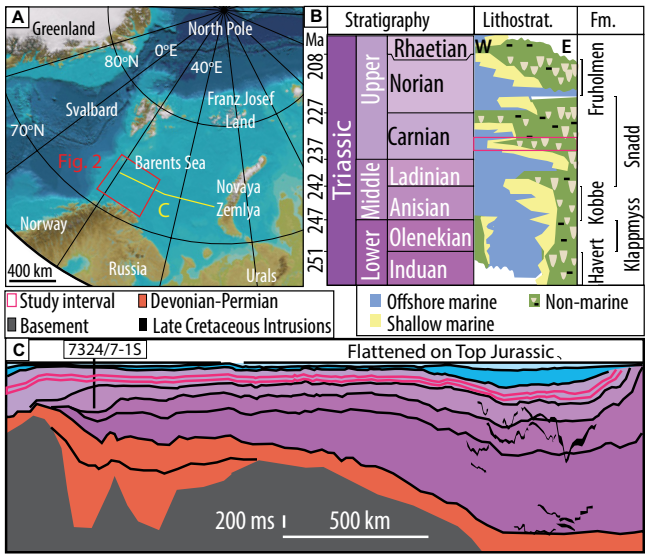

Figure 1. Area and stratigraphic context of study, Barents Sea region. A,B: Regional setting of modern Barents Sea (A), hosting Boral Ocean in Triassic, a period when basin was dominated by several phases of delta progradation (B). C: Regional cross section shows continuity of study interval (pink box within Carnian interval in B)—stretching beyond limits of our data set to west and toward Novaya Zemlya in east. Well 7324/7-1S was one of several wells used to tie the stratigraphic intervals to regional seismic profiles and 3-D seismic cubes (data were made available by the Norwegian Petroleum Directorate). The regional seismic section is flattened on the regional seismic reflector tied to the top of the Jurassic package. Black lines are formation boundaries. Triassic strata are marked with purple fill; Jurassic with blue fill. Westward migration of the main depocenter is initiated in Middle Triassic Ladinian interval, representing the lower part of the Snadd Formation. Lithostrat.—lithostratigraphy; Fm.—formation.

characteristic of meandering river systems forming in proximal parts of delta plains. The late Carnian shows similar but narrower channelized deposits, with both delta plains stretching across the basin (Klausen et al., 2015).

In this study, we restrict the TBO delta outline to the present shelf edge of the Barents Sea that overlies Triassic strata with deltaic deposits. Areas with time-equivalent deltaic deposits in eastern Greenland and the Canadian Sverdrup Basin (Hamann et al., 2005; Omma, 2009; Sømme et al., 2018) are excluded from the total area (see the GSA Data Repository[1]). This is a conservative approach to defining the actual potential size of the delta, as its basinward termination is not observed within the present outline. Prodeltaic, shallow marine, and bay deposits, however, interfinger with terrestrial deposits, demonstrating that this is a delta plain, not a floodplain (Klausen et al., 2015). The conservative estimate compensates for post-depositional tectonic stretching, which acted to extend the area over which the delta was originally deposited (Faleide et al., 2008). Restricted by the present shelf and the easternmost observations of terrestrial Carnian deposits, the TBO delta plain is measured to cover >1.65 × 10^6 km^2 (Fig. 3).

Despite subaerial exposure indicators such as paleosols, the TBO delta plain shows no signs of incision exceeding tens of meters (Klausen et al., 2015). The limited incision can explained by autogenic processes, which together with thick successions of terrestrial deposits attests to steady generation of accommodation (Fig. DR2 in the Data Repository) without periods of substantial degradation. This is an important characteristic of the TBO: its delta plain was overall net aggradational across its widespread extent.

COMPARISON TO MODERN AND ANCIENT COUNTERPARTS

Modern delta plains are geologically young and started prograding ~10 k.y. ago following eustatic sea-level rise in response to the retreat of ice coverage of the Last Glacial Maximum (LGM; Hanebuth et al., 2000; Berné et al., 2007). This contrasts with the TBO delta plain, where each progradational package approximates 2–5 m.y. (Klausen et al., 2015) and developed in a basin with steady accommodation. Comparing the areal extent of ancient and modern delta plains illustrates how different these geomorphological features can be at their mature and juvenile stages. The largest modern delta plain is associated with the Amazon River and covers ~1.08 × 10^5 km^2 (Fig. 4A), more than an order of magnitude smaller than the TBO delta plain.

Cenozoic glacio-eustatic lowstands caused delta plains to extend across the shallow marine areas now characterized as continental shelves (Hanebuth et al., 2000). The LGM represents the last of a series of lowstand stages and its deposits shaped modern shelves that consequently provide an estimate for the possible extent of delta plains developed during lowstand eustatic conditions. Pleistocene deposits of the northern Sunda shelf (southeast Asia) is an example of such a LGM delta plain, and within its stratigraphic record are indications of incision during pronounced eustatic sea-level lowering (Reijenstein et al., 2011). Large parts of LGM delta plains could therefore be net degradational. To avoid underestimation, the full possible extents of these LGM delta plains are considered (see the Data Repository). We exclude the arctic Barents and Kara shelves from LGM estimates because they were characterized by grounded ice sheets during glaciations (Jakobsson et al., 2016). The largest polar LGM shelf is located in the Chukchi Sea, covering ~8.26 × 10^5 km^2 or approximately half the size of the conservative TBO delta plain estimate (Fig. 4B). Outside of polar regions, the LGM shelf of the Gulf of Carpentaria (Australia) represents an area of 9.01 × 10^5 km^2, and the Yellow Sea represents an area of 8.56 × 10^5 km^2. The Sunda shelf is also large but comprised two distinct paleo-deltaic draining systems from the north and south (Reijenstein et al., 2011; Sathiamurthy and Voris, 2006), representing areas of 8.81 × 10^5 km^2 and 4.98 × 10^5 km^2 respectively, amounting to a combined area of 1.38 × 10^6 km^2. Despite our overestimates of the extents of LGM deltas, the TBO delta plain out-scales all.

Estimating the size of net-aggradational delta plains in the rock record is challenging because discrete delta plain boundaries are not readily constrained and commonly, due to post-depositional erosion, are incomplete. Tectonic overprint is also a limiting factor. An approximation is offered by comparison of the conservative outline for the TBO delta plain to interpreted outlines of formations with known large delta systems (Reijenstein et al., 2011; Broughton, 2016; Blum et al., 2017) and areas with extensive near-coast terrestrial deposition (Golonka, 2007) (Fig. 4C). Epicontinental seas, such as the Western Interior Basin (WIB, North America), were as much as 3.5 × 10^6 km^2 in extent and covered by terrestrial deposits at maximum regression, but comprised multiple discrete deltas not necessarily coeval or in a state of net aggradation (Bhattacharya et al., 2016). One large delta plain of the WIB in a net-aggradation state at maximum regression is represented by the Late Cretaceous McMurray Formation (western Canada). Although parts of this succession have been eroded, lower delta plain deposits observed in northern outcrops constrain parts of the deltaic part of this system (Broughton, 2016) and suggest that it is comparable in size (~1.02 × 10^6 km^2, based on outlines of Benyon et al. [2014]) to the TBO delta plain. Global paleogeographic reconstructions are poorly constrained for comparison with the TBO delta plain, but we note that some ancient coastal regions with terrestrial deposition approach conservative estimates of the extent of the TBO delta plain, all ~1.3 × 10^6 km^2 (Table DR1 in the Data Repository). These paleogeographic reconstructions (Golonka, 2007) do not discriminate between possible multiple deltaic systems, and go beyond

[1]GSA Data Repository item 2019177, supplementary text and figures for delta outline estimates, and table of outline values, is available online at http://www.geosociety.org/datarepository/2019/, or on request from editing@geosociety.org.

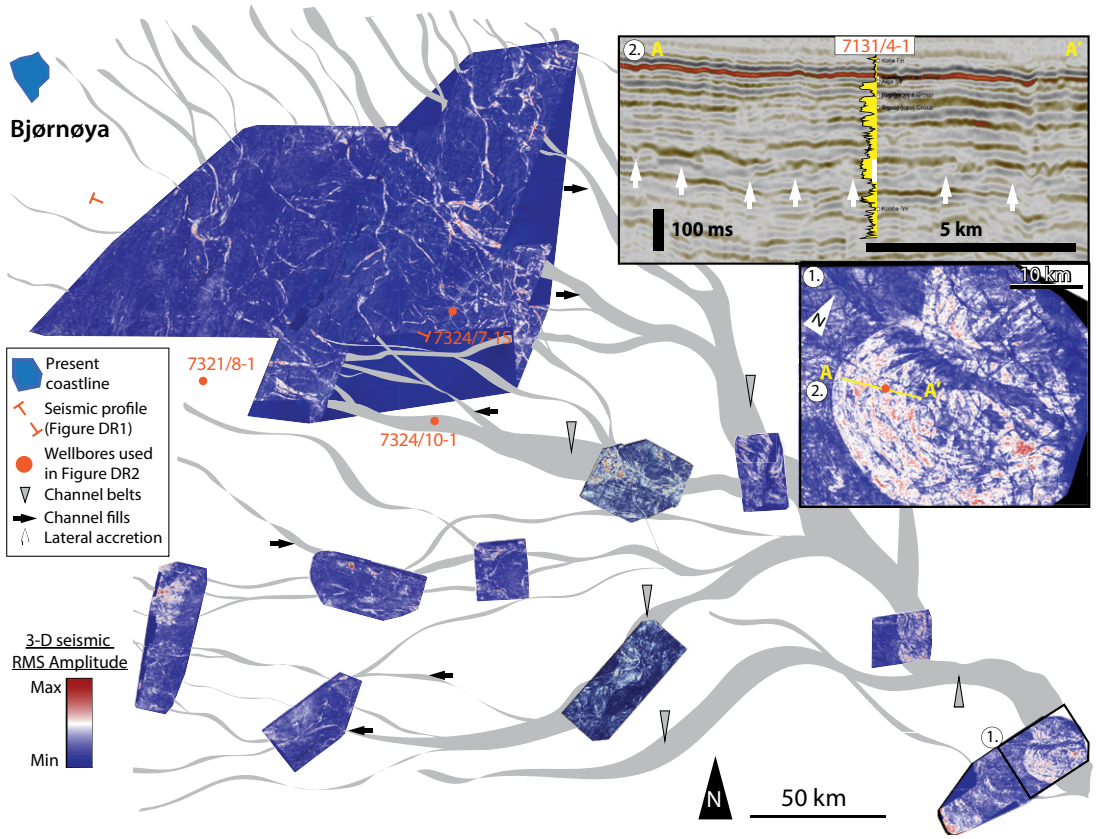

Figure 2. Distribution and character of channelized deposits on Triassic Boreal Ocean (TBO) delta plain. Root mean square (RMS) relative signal strength attribute maps are from 11 different three-dimensional seismic surveys (two surveys are merged in northwest) extracted on horizon equivalent to maximum regressive stage in early Carnian. Channelized deposits with lateral accretion characterize proximal parts of study area, whereas western parts are dominated by ribbon-shaped, elongated channelized deposits. Change from belt to ribbon approximate change from trunk river to distributary rivers in lower delta plain. Stratigraphic interval illustrated in these attribute maps is shown in Figure DR2 (see footnote 1). Scale bar applies to all surveys, and their relative distance is at scale, showing vast extent over which these channelized deposits are mappable. Island of Bjørnøya (Svalbard) is included for geographical reference. 3-D—three-dimensional; Max—maximum; Min—minimum. Inset 1 is close-up of lateral accretion surfaces characterizing channel belt deposits in eastern parts of study area. Inset 2 is cross section through meander bend in inset 1, showing lateral accretion surfaces relative to a well (7131/4-1 [data were made available by the Norwegian Petroleum Directorate]; gamma ray log in yellow, core interval in white) in near-angle offset two-dimensional seismic data.

the limited regions strictly defined as deltaic to include all terrestrial deposits. The largest area defined as deltaic (Golonka, 2007) is represented by the Kamienna Group in southeastern Europe, estimated to cover ~7.1 × 10^5 km^2.

Estimates of the TBO drainage area equal those of the largest in the world (Fig. 3); within this drainage area, Uralide topography likely surpassed that of the present, ranging from 4 to 6 km based on plate tectonic configurations (Puchkov, 2009). Although multiple smaller rivers likely contributed to the overall water and sediment discharge in the catchment, the presence of a single major trunk river system sourced from the southeast controlled sediment distribution to its associated delta plain (Klausen et al., 2015). High precipitation was facilitated by monsoonal climate (Hochuli and Vigran, 2010). Most important for extensive progradation was, however, a restricted paleobathymetric relief in front of the prograding delta (Fig. 4D). This relief has been defined using reconstructed prodeltaic clinoform surfaces following methods outlined in Klausen and Helland-Hansen (2018) and indicate a paleobathymetry of ~400 m (Fig. DR3). Although modern deltas could potentially migrate rapidly seaward in the more restricted water depths characterizing modern shelves (~120 m), created during late Holocene flooding (Hanebuth et al., 2000), this progradation would be halted by an increase in bathymetric relief ranging from 2000 m to 4000 m at their shelf edge (Fig. 4D), as deltas have repeatedly been throughout the Cenozoic. Steady accommodation and the likely absence of incision negate eustatically driven relative sea-level falls of ~50 m as inferred in the TBO basin by Haq et al. (1987). Although smaller-scale sea-level variations likely occurred and could, in addition to autocyclic delta lobe switching, explain parasequence-scale flooding surfaces, the large-scale delta architecture seems to have been controlled by transgressive-regressive cycles driven by normal progradation during prolonged sea-level highstand interrupted by transgressions at time scales of 10^6 yr. These transgressive-regressive cycles were likely caused by tectonically (Watts, 1982) and climatically (Hochuli and Vigran, 2010) driven variations in subsidence and sediment supply.

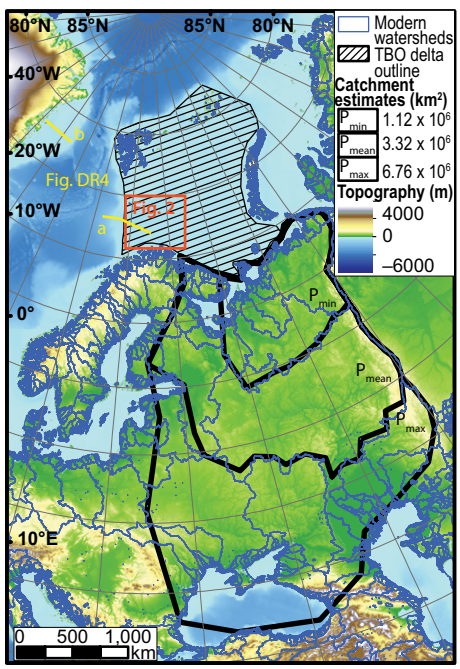

Figure 3. Areal extent and drainage estimates of Triassic Boreal Ocean (TBO) delta plain. Shown are conservative estimate of TBO delta plain outline, supported by previous studies (Miller et al., 2013; Klausen et al., 2015), and three potential catchment areas for this delta plain (minimum, mean, and maximum cases constrained by different paleogeographic scenarios discussed in Data Repository [see footnote 1]) compared to modern watersheds in same area. Yellow lines indicate position of published geologic sections (Hamann et al., 2005; Faleide et al., 2008), which indicate that TBO delta plain extended beyond conservative estimates used in present study (Fig. DR4 [see footnote 1]).

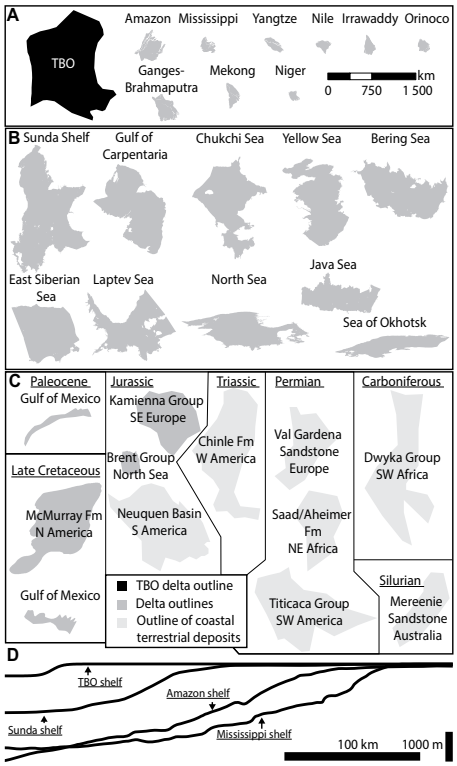

Figure 4. Comparison of surface area for large-scale deltas from different periods. A: Triassic Boreal Ocean (TBO) delta plain from Figure 3 compared to modern deltas: the Amazon River Delta, Brazil; the Mississippi River Delta, USA; The Yangtze River Delta, China; the Nile River Delta, Egypt; the Irrawaddy River Delta, Myanmar; the Orinoco River Delta, Venezuela; the Ganges-Brahmaputra River Delta, India and Bhangladesh; the Mekong River Delta, Vietnam; and the Niger River Delta, Nigeria. B: Possible Last Glacial Maximum (LGM) delta outlines: Sunda Shelf, Southeast Asia; Gulf of Carpentaria, Australia; Chukchi Sea, Laptev Sea, East Siberian Sea and Sea of Okhotsk, Russia; Bering Sea; Russia and USA; North Sea, northern Europe; Java Sea, Indonesia. C: Ancient terrestrial basins. All delta plain outline polygons are of similar scale, as presented in A. Fm—formation. D: Comparisons of reconstructed bathymetric profile from TBO (Fig. DR3 [see footnote 1]) to some modern counterparts. Projection and constraints on delta outlines and bathymetry are discussed in Data Repository (see footnote 1).

CONCLUSIONS AND IMPLICATIONS

River systems in the Boreal Ocean shaped the largest delta plain in Earth's history because of their large continental drainage area in northern Pangea, high sediment supply due to a recent and partly active orogeny, monsoonal rainfall facilitating high water discharge, a shallow marine basin, and relatively stable global sea levels. Some of these factors were specific to the TBO, especially paleobathymetry, while other factors are shared with modern and ancient counterparts. Delta plains of similar scale may have formed in ancient times, only to be destroyed in the rock cycle, but delta plains of this scale normally form on passive margins with relatively high preservation potential (Woodcock, 2004).

We conclude that (1) compared to a wide range of delta plains, some of which are likely composed of multiple river systems, the largest delta plain in Earth's history developed in the TBO of northern Pangea; (2) widespread delta plains require high sediment input from a large drainage area, but the most important prerequisite for the TBO was the shallow marine basin it prograded into; and (3) thick successions of nonmarine deposits indicate prolonged sea-level highstand uninterrupted by significant shoreline translocations, negating glacially driven eustatic changes and supporting a persistent Triassic greenhouse setting (Miller et al., 2005).

The TBO delta plain comprises a delta plain end member unaffected by anthropogenic factors and major fluctuations in global sea level—illustrating how extensive progradation and net land gain characterize delta progradation. Despite profound differences, the character of the TBO delta plain and associated river system resemble Quaternary counterparts in terms of delta plain development, demonstrating that discharge and equilibrium profiles control depositional styles in modern and ancient times alike. Although partly countered by high global sea level, increased river discharge from climatic change (Meehl et al., 2005) can potentially facilitate future TBO delta plain equivalents under prolonged interglacial conditions (Rahmstorf, 2007). Their extent will however be restricted by bathymetric relief, current plate-tectonic distributions, and topographic hinterland relief, lowering the likelihood for out-scaling the TBO delta plain.

ACKNOWLEDGMENTS

This study was funded in full by the Research Council of Norway through the ISBAR (Source-to-Sink of the Triassic Barents Sea) project, grant number 267689. Open Access was made possible with support from the University in Bergen and the ISBAR project. We are grateful for access to seismic data provided by TGS-Nopec (Oslo, Norway) and the Norwegian Petroleum Directorate, and academic software licenses provided by Schlumberger and Esri (California, USA). Marina Rabineau, three anonymous reviewers, and editor Mark Quigley are gratefully thanked for many thoughtful comments and suggestions that improved the manuscript considerably.

REFERENCES CITED

Archer, D., and Ganopolski, A., 2005, A movable trigger: Fossil fuel CO_2 and the onset of the next glaciation: Geochemistry Geophysics Geosystems, v. 6, Q05003, https://doi.org/10.1029/2004GC000891.

Benyon, C., Leier, A., Leckie, D.A., Webb, A., Hubbard, S.M., and Gehrels, G., 2014, Provenance of the Cretaceous Athabasca Oil Sands, Canada: Implications for continental-scale sediment transport: Journal of Sedimentary Research, v. 84, p. 136–143, https://doi.org/10.2110/jsr.2014.16.

Bernardi, M., Gianolla, P., Petti, F.M., Mietto, P., and Benton, M.J., 2018, Dinosaur diversification linked with the Carnian Pluvial Episode: Nature Communications, v. 9, 1499, https://doi.org/10.1038/s41467-018-03996-1.

Berné, S., Jouet, G., Bassetti, M.A., Dennielou, B., and Taviani, M., 2007, Late Glacial to Preboreal sea-level rise recorded by the Rhône deltaic system (NW Mediterranean): Marine Geology, v. 245, p. 65–88, https://doi.org/10.1016/j.margeo.2007.07.006.

Bhattacharya, J.P., Copeland, P., Lawton, T.F., and Holbrook, J., 2016, Estimation of source area, river paleo-discharge, paleoslope, and sediment budgets of linked deep-time depositional systems and implications for hydrocarbon potential: Earth-Science Reviews, v. 153, p. 77–110, https://doi.org/10.1016/j.earscirev.2015.10.013.

Blum, M.D., and Roberts, H.H., 2009, Drowning of the Mississippi Delta due to insufficient sediment supply and global sea-level rise: Nature Geoscience, v. 2, p. 488–491, https://doi.org/10.1038/ngeo553.

Blum, M.D., Milliken, K.T., Pecha, M.A., Snedden, J.W., Frederick, B.C., and Galloway, W.E., 2017, Detrital-zircon records of Cenomanian, Paleocene, and Oligocene Gulf of Mexico drainage integration and sediment routing: Implications for scales of basin-floor fans: Geosphere, v. 13, p. 2169–2205, https://doi.org/10.1130/GES01410.1.

Broughton, P.L., 2016, Alignment of fluvio-tidal point bars in the middle McMurray Formation: Implications for structural architecture of the Lower Cretaceous Athabasca Oil Sands Deposit, northern Alberta: Canadian Journal of Earth Sciences, v. 53, p. 896–930, https://doi.org/10.1139/cjes-2015-0137.

Eide, C.H., Klausen, T.G., Katkov, D., Suslova, A.A., and Helland-Hansen, W., 2017, Linking an Early Triassic delta to antecedent topography: Source-to-sink study of the southwestern Barents Sea margin: Geological Society of America Bulletin, v. 130, p. 263–283, https://doi.org/10.1130/B31639.1.

Faleide, J.I., Tsikalas, F., Breivik, A.J., Mjelde, R., Ritzmann, O., Engen, Ø., Wilson, J., and Eldholm, O., 2008, Structure and evolution of the continental margin off Norway and the Barents Sea: Episodes, v. 31, p. 82–91.

Golonka, J., 2007, Late Triassic and Early Jurassic palaeogeography of the world: Palaeogeography, Palaeoclimatology, Palaeoecology, v. 244, p. 297–307, https://doi.org/10.1016/j.palaeo.2006.06.041.

Greb, S.F., DiMichele, W.A., and Gastaldo, R.A., 2006. Evolution and importance of wetlands in Earth History, *in* Greb, S.F., and DiMichele, W.A., eds., Wetlands through Time: Geological Society of America Special Paper 399, p. 1–40, https://doi.org/10.1130/2006.2399(01).

Hamann, N.E., Whittaker, R.C., and Stemmerik, L., 2005, Geological development of the Northeast Greenland shelf, *in* Doré, A.G., and Vining, B.A., eds., Petroleum Geology: North-West Europe and Global Perspectives—Proceedings of the 6th Geology Conference: Geological Society of London Petroleum Geology Conference Series 6, p. 887–902, https://doi.org/10.1144/0060887.

Hanebuth, T., Stattegger, K., and Grootes, P.M., 2000, Rapid flooding of the Sunda Shelf: A late-glacial sea-level record: Science, v. 288, p. 1033–1035, https://doi.org/10.1126/science.288.5468.1033.

Haq, B.U., Hardenbol, J.A.N., and Vail, P.R., 1987, Chronology of fluctuating sea levels since the Triassic: Science, v. 235, p. 1156–1167, https://doi.org/10.1126/science.235.4793.1156.

Hochuli, P.A., and Vigran, J.O., 2010, Climate variations in the Boreal Triassic—Inferred from

palynological records from the Barents Sea: Palaeogeography, Palaeoclimatology, Palaeoecology, v. 290, p. 20–42, https://doi.org/10.1016/j.palaeo.2009.08.013.

Jakobsson, M., et al., 2016, Evidence for an ice shelf covering the central Arctic Ocean during the penultimate glaciation: Nature Communications, v. 7, 10365, https://doi.org/10.1038/ncomms10365.

Klausen, T.G., and Helland-Hansen, W., 2018, Methods for restoring and describing ancient clinoform surfaces: Journal of Sedimentary Research, v. 88, p. 241–259, https://doi.org/10.2110/jsr.2018.8.

Klausen, T.G., Ryseth, A.E., Helland-Hansen, W., Gawthorpe, R., and Laursen, I., 2015, Regional development and sequence stratigraphy of the Middle to Late Triassic Snadd Formation, Norwegian Barents Sea: Marine and Petroleum Geology, v. 62, p. 102–122, https://doi.org/10.1016/j.marpetgeo.2015.02.004.

Meehl, G.A., Arblaster, J.M., and Tebaldi, C., 2005, Understanding future patterns of increased precipitation intensity in climate model simulations: Geophysical Research Letters, v. 32, L18719, https://doi.org/10.1029/2005GL023680.

Miller, E.L., Soloviev, A.V., Prokopiev, A.V., Toro, J., Harris, D., Kuzmichev, A.B., and Gehrels, G.E., 2013, Triassic river systems and the paleo-Pacific margin of northwestern Pangea: Gondwana Research, v. 23, p. 1631–1645, https://doi.org/10.1016/j.gr.2012.08.015.

Miller, K.G., Kominz, M.A., Browning, J.V., Wright, J.D., Mountain, G.S., Katz, M.E., Sugarman, P.J., Cramer, B.S., Christie-Blick, N., and Pekar, S.F., 2005, The Phanerozoic record of global sea-level change: Science, v. 310, p. 1293–1298, https://doi.org/10.1126/science.1116412.

Omma, J.E., 2009, Provenance of Late Paleozoic and Mesozoic sediment to key Arctic basins: Implications for the opening of the Arctic Ocean [Ph.D. thesis]: Cambridge, UK, University of Cambridge, 235 p.

Paterson, N.W., and Mangerud, G., 2017, Palynology and depositional environments of the Middle–Late Triassic (Anisian–Rhaetian) Kobbe, Snadd and Fruholmen formations, southern Barents Sea, Arctic Norway: Marine and Petroleum Geology, v. 86, p. 304–324, https://doi.org/10.1016/j.marpetgeo.2017.05.033.

Puchkov, V.N., 2009, The evolution of the Uralian orogen, *in* Murphy, J.B., et al., eds., Ancient Orogens and Modern Analogues: Geological Society of London Special Publication 327, p. 161–195, https://doi.org/10.1144/SP327.9.

Rahmstorf, S., 2007, A semi-empirical approach to projecting future sea-level rise: Science, v. 315, p. 368–370, https://doi.org/10.1126/science.1135456.

Reijenstein, H.M., Posamentier, H.W., and Bhattacharya, J.P., 2011, Seismic geomorphology and high-resolution seismic stratigraphy of inner-shelf fluvial, estuarine, deltaic, and marine sequences, Gulf of Thailand: American Association of Petroleum Geologists Bulletin, v. 95, p. 1959–1990, https://doi.org/10.1306/03151110134.

Sathiamurthy, E., and Voris, H.K., 2006, Maps of Holocene sea level transgression and submerged lakes on the Sunda Shelf: Natural History Journal of Chulalongkorn University, Suppl. 2, p. 1–44.

Syvitski, J.P.M., and Saito, Y., 2007, Morphodynamics of deltas under the influence of humans: Global and Planetary Change, v. 57, p. 261–282, https://doi.org/10.1016/j.gloplacha.2006.12.001.

Syvitski, J.P.M., et al., 2009, Sinking deltas due to human activities: Nature Geoscience, v. 2, p. 681–686, https://doi.org/10.1038/ngeo629.

Sømme, T.O., Doré, A.G., Lundin, E.R., and Tørudbakken, B.O., 2018, Triassic–Paleogene paleogeography of the Arctic: Implications for sediment routing and basin fill: American Association of Petroleum Geologists Bulletin, v. 102, p. 2481–2517, https://doi.org/10.1306/05111817254.

Vigran, J.O., Mangerud, G., Mørk, A., Worsley, D., and Hochuli, P.A., 2014, Palynology and Geology of the Triassic Succession of Svalbard and the Barents Sea: Geological Survey of Norway Special Publication 14, 274 p.

Watts, A.B., 1982, Tectonic subsidence, flexure and global changes of sea level: Nature, v. 297, p. 469–474, https://doi.org/10.1038/297469a0.

Woodcock, N.H., 2004, Life span and fate of basins: Geology, v. 32, p. 685–688, https://doi.org/10.1130/G20598.1.

Woodroffe, C.D., Nicholls, R.J., Saito, Y., Chen, Z., and Goodbred, S.L., 2006, Landscape variability and the response of Asian megadeltas to environmental change, *in* Harvey, N., ed., Global Change and Integrated Coastal Management: The Asia-Pacific Region: Dordrecht, Netherlands, Springer, p. 277–314, https://doi.org/10.1007/1-4020-3628-0_10.

Printed in USA